J Mater Sci (2006) 41:6973–6977
DOI 10.1007/s10853-006-0219-0

An investigation of the effects of mix strength on the fracture and fatigue behavior of concrete mortar

J. Lou · K. Bhalerao · A. B. O. Soboyejo · W. O. Soboyejo

Received: 20 February 2003 / Accepted: 21 February 2005 / Published online: 16 September 2006

Abstract This paper examines the effects of mix compressive strength (30, 35 and 40 MPa) on the fracture initiation toughness, resistance-curve behavior and fatigue crack growth behavior of concrete mortar. The fracture initiation toughness and the resistance-curve behavior are shown to increase with increasing mix strength. The observed resistance-curve behavior is then attributed largely to the effects of ligament bridging, which are predicted using small- and large-scale bridging models. In contrast, the fatigue crack growth resistance is shown to decrease with increasing mix strength. An extended multiparameter framework was used for the modeling of fatigue crack growth. Finally, the implications of the results are discussed for the design of concrete mixtures with attractive combinations of strength, fracture toughness and fatigue crack growth resistance.

Introduction

Significant efforts have been made to understand the toughening components that contribute to the fracture toughness of concrete [1–4]. These studies have shown that stable crack growth in concrete is generally associated with the formation of bridging ligaments and anti-shielding/shielding microcracking zones. However, a simple modeling framework for the prediction of toughening/resistance-curve behavior in concrete mortar is yet to be developed.

Meanwhile, sub-critical crack growth associated with cyclic loading due to freeze-thaw cycles [5], mechanical loading by traffic, and wind loading in concrete structures may occur at stress levels that are well below the critical conditions required for failure under monotonic loading [6]. Moreover, a wide range of parameters may influence fatigue crack growth rates in concrete [7, 8]. These include: the stress intensity factor range, ΔK; stress ratio, R; maximum stress intensity factor, K_{max}; and relative humidity [7].

This paper presents a simple small- and large-scale bridging framework for the modeling of toughening due to ligament bridging in concrete mortar. An extended multiparameter framework is also presented for the modeling of fatigue crack growth in concrete mortar. The models are applied to the prediction of resistance-curve behavior and fatigue crack growth behavior in concrete mortar with strength levels of 30, 35 and 40 MPa. Finally, the implications of the results are discussed for the design of durable concrete structures.

Materials and experimental procedures

The concrete material that was used in this study was produced at The Ohio State University, Columbus, OH. Concrete mixes with nominal compressive strength levels of 30, 35 and 40 MPa were obtained by the mixing of aggregates and cement in the ratios shown in Table 1.

J. Lou · W. O. Soboyejo (✉)
Princeton Materials Institute, and the Department of Mechanical and Aerospace Engineering, Princeton University, Princeton, NJ 08544, USA
e-mail: soboyejo@princeton.edu

K. Bhalerao · A. B. O. Soboyejo
Department of Food, Agricultural and Biological Engineering, and the Department of Aerospace Engineering, The Ohio State University, Columbus, OH 43210, USA

Table 1 Nominal composition of the three types of concrete

Mix (30 MPa)	Mix (35 MPa)	Mix (40 MPa)
Cement: Type I; 1 part; 456.59 kg/m^3 Coarse aggregate: irregular gravel; 2.672 parts; 1220.23 kg/m^3 Fine aggregate: well-graded sand; 0.890 parts; 406.74 kg/m^3 Workability: medium Water/cement ratio: 0.416; 190.18 lit/m^3	Cement: Type I; 1 part; 513.39 kg/m^3 Coarse aggregate: irregular gravel; 2.255 parts; 1172.42 kg/m^3 Fine aggregate: well-graded sand; 0.751 parts; 390.47 kg/m^3 Workability: medium Water/cement ratio: 0.378; 196.84 lit/m^3	Cement: Type I; 1 part; 609.26 kg/m^3 Coarse aggregate: irregular gravel; 1.808 parts; 1101.57 kg/m^3 Fine aggregate: well-graded sand; 0.602 parts; 360.19 kg/m^3 Workability: medium Water/cement ratio: 0.338; 206.37 lit/m^3

After mixing, the concrete was allowed to harden for at least 28 days before conducting the resistance-curve and fatigue crack growth experiments at Princeton University, Princeton, NJ.

The resistance-curve and the fatigue crack growth experiments were conducted on single edge notched bend specimens (SENB) in a servo-hydraulic testing machine. Crack growth during the experiments was monitored using a notch-mouth clip gauge that was attached to the notch mouth using knife-edges and a Questar telescope (resolution of ~2.5 μm) that was connected to a video monitoring unit.

For the resistance-curve tests, low initial loads corresponding to a stress intensity factor of ~0.2 MPa√m, were applied initially. After each incremental crack growth step, the loads were increased in steps of ~5% until stable crack growth occurred. Following each incremental crack growth step, the crack/microstructure interactions were examined and photographed with an optical microscope. The above procedure was then repeated until catastrophic failure occurred.

In the case of fatigue crack growth experiments, initial stress intensity factor ranges of ~0.3 MPa√m were increased in 5–10% steps until stable crack growth was detected by the notch-mouth clip gauge (compliance technique) after ~ 10,000–50,000 cycles. The load ranges were then maintained constant, as the crack length increased beyond the near-threshold regime. In this way, fatigue crack growth rate data were obtained under increasing ΔK condition.

After final fracture, the fracture surfaces of the fracture and fatigue specimens were examined under a light microscope. This was done to reveal the underlying three-dimensional crack paths and fracture modes.

Results and discussion

Resistance curve behavior

The measured resistance curves obtained for the three concrete specimens are presented in Fig. 1. This shows that initiation toughness and resistance-curve behavior improve with increased mixture strength between 30 and 40 MPa. The resistance-curve behavior of the 40 MPa concrete is

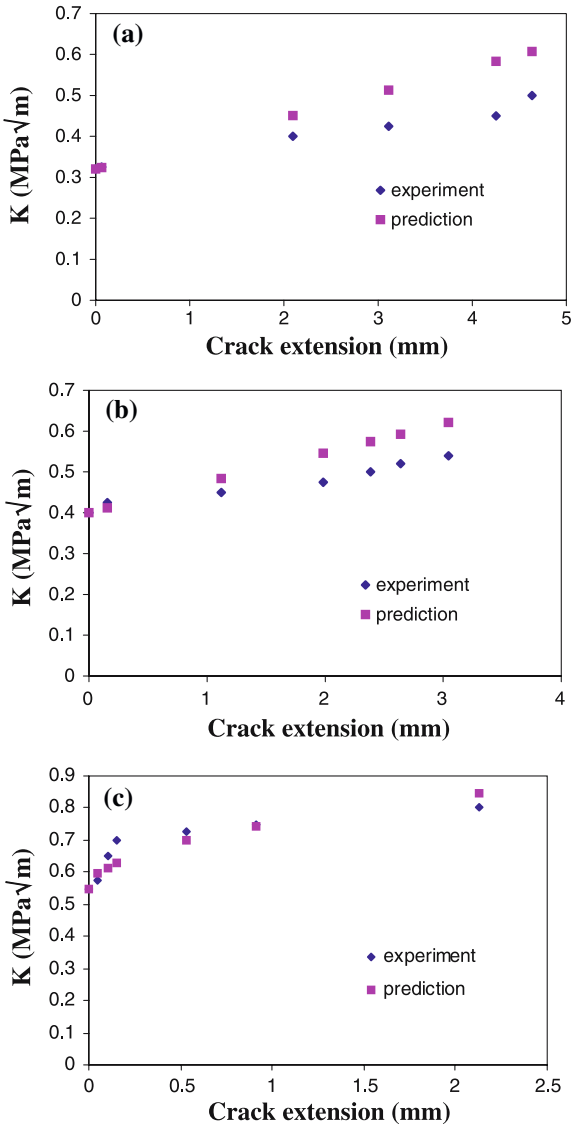

Fig. 1 Comparison of the experimental and predicted resistance-curve behavior for concrete with the strength levels of: (**a**) 30 MPa; (**b**) 35 MPa; (**c**) 40 MPa

considerably better than that of the 30 and 35 MPa concrete. However, the amount of stable crack growth increases with decreasing concrete strength (Fig. 1). Typical fracture modes are shown in Fig. 2(a)–(c) for the three strength levels. These show tortuous crack paths and rough fracture surfaces in all of the three cases.

To model the observed resistance-curve behavior, a combination of the small- and large-scale bridging concepts was explored [9]. For the initial problem of small-scale bridging, Budiansky [10] and Tada et al. [11] proposed a solution for the toughening estimation. This gives rise to the toughening ratio, λ_{ssb}, due to crack bridging as:

$$\lambda_{ssb} = \frac{K}{K_m} = 1 + \sqrt{\frac{2}{\pi}}\frac{f}{K_m}\int_0^L \frac{\alpha\sigma(x)}{\sqrt{x}}\mathrm{d}x \quad (1)$$

where α is a constraint factor, $\sigma(x)$ is the bridging traction, x is the distance from the crack face behind the crack-tip, and L is bridging length. For subsequent large-scale bridging, the shielding due to large-scale bridging, ΔK_{lsb}, is given by Bloyer et al. [12] and Li and Soboyejo [13] as:

$$\Delta K_{lsb} = \int_L \alpha\sigma(x)h(a,x)\mathrm{d}x \quad (2)$$

where L is the length of the bridge zone, α is a constraint factor, $\sigma(x)$ is a traction function along the bridge zone, and $h(a,x)$ is a weight function given by Fett and Munz [14].

Using parameters summarized in Table 2, the resistance-curves were predicted for stable crack growth in the small-scale bridging ($\Delta a < 0.5$ mm) and large-scale bridging ($\Delta a \geq 0.5$ mm) regimes. The results of the predictions are presented in Fig. 1(a)–(c). The predictions are generally in good agreement with the measured resistance curves obtained for concrete with different strength levels. The small-scale bridging models, therefore, captured the early part of the resistance-curves, while the large-scale bridging model provided good predictions of subsequent resistance-curve behavior.

Table 2 Summary of basic mechanical properties and parameters used in the small- and large-scale bridging model

Mechanical Property and Parameters	30 MPa Concrete	35 MPa Concrete	40 MPa Concrete
Young's modulus (MPa)	31220	33721	36049
Compressive strength (MPa)	30	35	40
Volume fraction of ligaments, V_l	0.1	0.1	0.1

Fatigue crack growth behavior

A summary of the fatigue crack growth rate data obtained from the current study is presented in Fig. 3. These show data obtained for stress ratios, R, of 0.1 and 0.25 for concrete mortar samples with different strength levels. The data exhibit some scatter, which is consistent with the heterogeneous structure of the concrete materials that were studied. The typical fracture mode (Fig. 4(a)–(c)) for the fatigue samples is transgranular fracture with less rough fracture surfaces as we saw in R-curve behavior sample.

The dependence of fatigue crack growth rate, da/dN, on the crack driving force is often modeled using the Paris-Erdogan law [15]. However, in many cases, a single crack driving force, such as ΔK, may not adequately account for

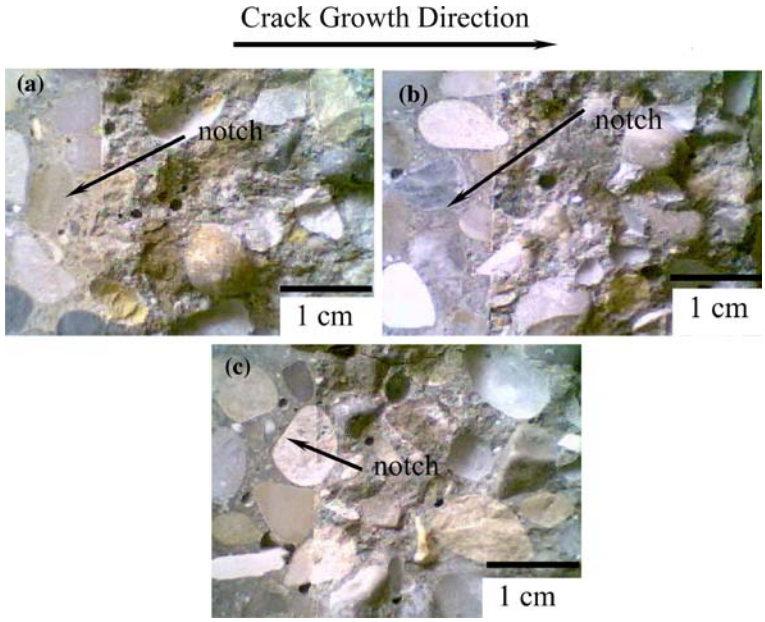

Fig. 2 Typical fracture modes of resistance-curve behavior of concrete mortar with strength levels of (**a**) 30 MPa; (**b**) 35 MPa and (**c**) 40 MPa

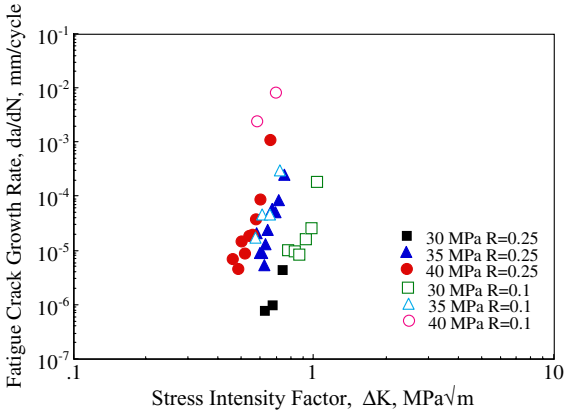

Fig. 3 Fatigue crack growth rate data obtained from concrete with strength levels of 30, 35 and 40 Mpa

all the parameters that influence fatigue crack growth. Hence, it is common to express the fatigue crack growth rate, d*a*/d*N*, as functions of at least two parameters [16]. The most commonly used two-parameter law is:

$$\frac{da}{dN} = A(\Delta K)^m (K_{max})^n \quad (3)$$

where A, m and n are empirical constants, ΔK is the stress intensity factor range, and K_{max} is the maximum stress intensity factor range. Thus, this simplified multiparameter law [17] was applied to the characterization of fatigue crack growth in the present study. The results are presented in Table 3. These show that the fatigue crack growth rates are controlled primarily by ΔK, and to a lesser extent by K_{max}. It is important to note that the effects of stress ratio

Table 3 Summary of multiparameter constants

Mix Strength (MPa)	A	m	n	r^2
30	–7.48	5.18	1.36	0.97
35	–7.99	–0.60	3.09	0.84
40	6.3	27.7	–7.78	0.87

are fully accounted for by K_{max} effects. Hence, a two parameter approach captures both the effects of ΔK and R.

Implications

The above results show that the concrete mixes with improved strength and fracture toughness do not necessarily have improved fatigue crack growth resistance. This is due largely to the fact that the bridging zones are degraded under cyclic loading. Hence, the shielding contributions from ligaments (which are largely present under monotonic loading) are much less effective under cyclic loading. In any case, the current results suggest that an optimum approach to the design of durable concrete mortar is one that involves the design of mixes with a balance of strength, fracture toughness and fatigue crack growth resistance.

Concluding remarks

Resistance Curve Behavior and fatigue crack growth have been studied in three grades of concrete with strength levels of 30, 35 and 40 MPa. The following conclusions

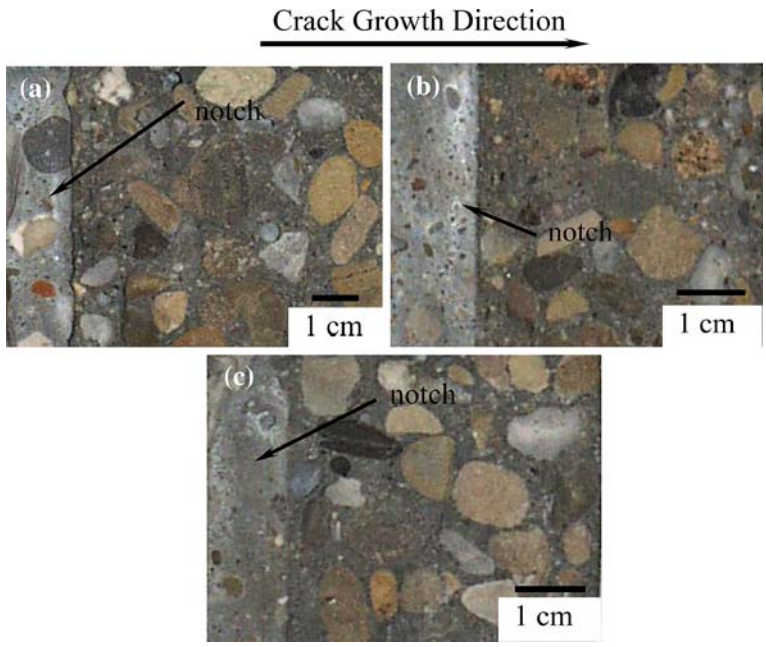

Fig. 4 Typical fatigue fracture modes of concrete mortar with strength levels of (**a**) 30 MPa; (**b**) 35 MPa and (**c**) 40 MPa

have been reached from the combined experimental and theoretical study:

1. A combination of small- and large-scale ligament bridging model was used to predict the resistance-curve behavior of concrete with strength levels of 30, 35 and 40 MPa. The predictions are in good agreement with the experimental data.
2. A multiparameter method can be used to relate the effects of multiple variables on fatigue crack growth in concrete. The power law expression, which is a logical extension of the Paris-Erdogan law, relates fatigue crack growth rate to stress intensity factor range, ΔK, maximum stress intensity factor, K_{max}.
3. Although the fracture toughness and resistance curve behavior improved with increasing mix strength, the fatigue crack growth resistance of the selected concrete shows the opposite trends. This suggests that a balanced approach is needed in the design of concrete mixtures with the required combination of strength, fracture toughness and fatigue crack growth resistance.

Acknowledegments The research is supported by The Division of Mechanics and Materials of The National Science Foundation, with Dr. Oscar Dillon and Dr. Ken Chong as Program Monitors. Appreciation is also extended to Dr. Dan Davis for his encouragement and support of this work.

References

1. Karihaloo BL, Nallathambi P (1989) Cement Concr Res 19:603
2. Jeng Y-S, Shah SP (1985) J Eng Mech 111:1227
3. Bazant ZP, Kim JK, Pfeiffer PA (1986) J Struct Eng 112:289
4. RILEM FMC-50, RILEM, ''Materiux et Constructions'' 18:287
5. Marchand J, Pleau R, Gagne R (1995) In: Skalny J, Mindess S (eds) Material Science of concrete IV, Acers, pp 283
6. Nordby Gene M (1958) ACI J 55:191
7. Bhalerao K, Shen W, Soboyejo ABO, Soboyejo WO (2003) Int J Concr Cement Compos 25:607
8. Bazant ZP, Xu K (1991) ACI J 88:390
9. Lou J, Soboyejo WO (2001) Metallurg Mater Trans 32A:325
10. Budiansky B, Amazigo JC, Evans AG (1988) J Mech Phys Solids 36:167
11. Tada H, Paris PC, Irwin GR (1999) The stress analysis of cracks handbook. American Society of Mechanical Engineers, New York, NY
12. Bloyer DR, Venkateswara Rao KT, Ritchie RO (1998) Metall Mater Trans A 29A:2483
13. Li M, Soboyejo WO (2000) Metall Mater Trans A 31A:1385
14. Fett T, Munz D (1994) Stress intensity factors and weight functions for one-dimensional cracks. Institut fur Materialforschung, Kernforschungszentrum, Karlsryhe, Germany
15. Paris PC, Gomez M, Anderson WE (1961) Trend Engineer 13:9
16. Soboyejo WO, Shen W, Lou J, Mercer C, Sinha V, Soboyejo ABO (2002) Int J Fatig 24:69